

**AN ANALYTICAL INVESTIGATION OF FOUR-LAYER DIELECTRIC OPTICAL FIBERS WITH AU NANO-COATING — A COMPARISON WITH THREE-LAYER OPTICAL FIBERS**

**F. A. Rahman**

Faculty of Engineering and Science  
Universiti Tunku Abdul Rahman  
Setapak 53300, Malaysia

**P. K. Choudhury, D. Kumar, and Z. Yusoff**

Faculty of Engineering  
Multimedia University  
Cyberjaya 63100, Malaysia

**Abstract**—An analytical investigation has been presented of Au nano-coated dielectric optical fibers. The propagation constants of different transverse TE and hybrid EH modes are obtained corresponding to varying nano-coating thickness. It has been observed that the Au-layer has its profound effect on the number of propagating modes in the fiber, and the number of sustained modes is much reduced with the increase in Au-layer thickness. For the sake of comparative investigation, the modal behavior of three-layer dielectric fibers is also taken into account together with the Au nano-coated four-layer fiber. It is reported that the Au-layer has the effect of mode proliferation with simultaneous reduction in their propagation constant values.

---

Corresponding author: F. A. Rahman (faidzar@utar.edu.my).

## 1. INTRODUCTION

Optical waveguides have their importance in versatile applications, viz. communication purposes, sensing technology as well as integrated optical devices. In this context, guides with varieties of new forms of geometrical cross-sections and/or composite materials have been put into applications [1–10].

The investigation of electromagnetic (EM) behavior of conventional optical fibers does not involve much difficulty. Studies related to many types of optical fibers with different refractive index (RI) profiles and different numbers of claddings have appeared in the literature [11–14]. However, these investigations mostly implemented oversimplified assumptions. A strict analytical approach becomes forbiddingly difficult to tackle with, which is essentially owing to the presence of multiple claddings in the fiber.

Application of optical waveguides in sensing technology has now been well-established [15–19]. In this context, fibers with gold (Au) nano-coating are of special mention as these are much advantageous in chemical sensing; Au nano-particles can efficiently react with the ambient environment [20, 21]. By using such Au-coated fibers, the optical sensitivity of the system can also be enhanced on demand by controlling the thickness of the nano-layer coating. Further, these fibers are considered to be quite useful even for the detection of weak chemical reactions without sacrificing the measurement sensitivity.

In Brillouin-based distributed fiber-optic sensors, fibers with multiple layers have also been used as efficient sensing mediums to sense both strain and temperature [22–24]. In order to perform a thorough investigation of the sensing aspects of Au-coated fibers, the knowledge of their modal characteristics is vital in respect of their propagation constants [25]. The present communication aims to report an analytical investigation of optical fibers with emphasis on their modal behavior. The fiber structure is essentially a multilayered dielectric fiber loaded with a metallic nano-layer. There is a considerable amount of RI difference between the different regions of the fiber. This makes the use of Maxwell's field equations necessary.

The analysis essentially requires the estimation of fields in the different fiber regions. Strictly speaking, the fields in the metallic region must be vanishing. However, as the relevant fiber region is nano-sized thick, there must be some amount of field present in that region, and for this purpose, Hankel function is particularly implemented. Finally, the field in the Au-coated region is taken to be the linear combination of the modified Bessel function of the second kind and Hankel function [26]. With these assumptions, a rigorous analytical

treatment is performed for the Au-coated fiber emphasizing the modal aspects. Also, in order to visualize the effect of additional nano-layer of gold upon the dielectric fiber, a comparative modal analysis of the Au-coated fiber and a three-layer dielectric fiber is also presented.

## 2. ANALYTICAL TREATMENT

We consider the meridional cross-section of a four-layer fiber of which the third layer is assumed to be loaded with Au-coated nano-layer. The outermost layer is considered as the infinitely extended free-space having an RI of  $n_4 = 1$ . RIs of the other different layers are represented as  $n_1$ ,  $n_2$ , and  $n_3$  with  $n_1 > n_2 > n_3$ . The analysis of the fiber structure essentially needs the use of the cylindrical polar coordinate system  $(\rho, \phi, z)$ ;  $z$ -axis being the optical axis of the fiber along which the propagation takes place. There are three interfaces in the fiber separating the different regions, and the parametric boundaries of the different layers are considered to be  $\rho = \rho_1$ ,  $\rho = \rho_2$  and  $\rho = \rho_3$  with  $\rho_1 < \rho_2 < \rho_3$ . Thus, the region with  $\rho_3 - \rho_2 (= \delta)$  is assumed to have the Au nano-layer coating.

Solutions of the wave equation with cylindrical symmetry for axial components of the electric/magnetic fields  $E_z$  and  $H_z$  are sought for the four regions, and then matched at the interfaces for continuity conditions. The wave equation is

$$\frac{\partial^2 \psi}{\partial \rho^2} + \frac{1}{\rho} \frac{\partial \psi}{\partial \rho} + \frac{1}{\rho^2} \frac{\partial^2 \psi}{\partial \phi^2} + q^2 \psi = 0 \quad (1)$$

where  $\psi$  stands for either  $E_z$  or  $H_z$ , as the case may be. Also,  $q^2 = \omega^2 \mu \varepsilon - \beta^2$  with  $\omega$  as the angular frequency of the wave in the unbounded medium,  $\beta$  as the axial component of the propagation constant, and  $\mu$  and  $\varepsilon$ , respectively, as the permeability and permittivity of the medium.

In order to compare the analytical results for the fibers with and without Au-coating, we consider the case of a three-layer fiber as well. As such, we now deal with the two situations individually, viz. Case I corresponding to the four-layer fiber with Au-coated nano-layer, and Case II corresponding to the three-layer dielectric fiber.

### 2.1. Case I: Fiber with Au-coating (Four-layer Fiber)

In the case of such a fiber, in the central core section, the solution can be taken in the form of Bessel function  $J_\nu(\cdot)$  of the first kind;  $\nu$  representing the azimuthal periodicity, which can take only discrete values. Essentially the symbol  $\nu$  represents the mode index. In

the outermost clad region, the field has a decaying character as one moves away from the fiber axis, and therefore, the solution can be best represented by the modified Bessel function  $K_\nu(\cdot)$  of the second kind. In the remaining two intermediate regions, the solutions must be formed by linear combinations — in the region next to the fiber core, by Bessel function of the first and the second kinds, i.e.,  $J_\nu(\cdot)$  and  $Y_\nu(\cdot)$ , and in the remaining region before the outermost clad, by the modified Bessel function of the second kind and Hankel function, i.e.,  $K_\nu(\cdot)$  and  $H_\nu^{(1)}(\cdot)$  [26]. Based on these considerations, the axial components of electric/magnetic fields in the different regions, illustrated by the suffices 1, 2, 3 and 4, of the fiber may be written as follows:

*Region I: core* ( $0 \leq \rho \leq \rho_1$ )

$$E_{z1} = C_1 J_\nu(\gamma_1 \rho) e^{j\nu\phi} \quad (2a)$$

$$H_{z1} = C_2 J_\nu(\gamma_1 \rho) e^{j\nu\phi} \quad (2b)$$

*Region II: inner cladding* ( $\rho_1 \leq \rho \leq \rho_2$ )

$$E_{z2} = \{C_3 J_\nu(\gamma_2 \rho) + C_4 Y_\nu(\gamma_2 \rho)\} e^{j\nu\phi} \quad (3a)$$

$$H_{z2} = \{C_5 J_\nu(\gamma_2 \rho) + C_6 Y_\nu(\gamma_2 \rho)\} e^{j\nu\phi} \quad (3b)$$

*Region III: Au coated-layer* ( $\rho_2 \leq \rho \leq \rho_3$ )

$$E_{z3} = \{C_7 K_\nu(\gamma_3 \rho) + C_8 H_\nu^{(1)}(\gamma_3 \rho)\} e^{j\nu\phi} \quad (4a)$$

$$H_{z3} = \{C_9 K_\nu(\gamma_3 \rho) + C_{10} H_\nu^{(1)}(\gamma_3 \rho)\} e^{j\nu\phi} \quad (4b)$$

*Region IV: outer cladding* ( $\rho \geq \rho_3$ )

$$E_{z4} = C_{11} K_\nu(\gamma_4 \rho) e^{j\nu\phi} \quad (5a)$$

$$H_{z4} = C_{12} K_\nu(\gamma_4 \rho) e^{j\nu\phi} \quad (5b)$$

In Eqs. (2a)–(5b),  $C_1$ – $C_{12}$  represent unknown constants to be determined by the boundary conditions. Also,  $\gamma_1$ ,  $\gamma_2$ ,  $\gamma_3$  and  $\gamma_4$  are the quantities corresponding to the different regions of the fiber; these parameters are defined as follows:

$$\gamma_1^2 = k_1^2 - \beta^2 = \omega^2 \mu \epsilon_1 - \beta^2 \quad (6a)$$

$$\gamma_2^2 = \beta^2 - k_2^2 = \beta^2 - \omega^2 \mu \epsilon_2 \quad (6b)$$

$$\gamma_3^2 = \beta^2 - k_3^2 = \beta^2 - \omega^2 \mu \epsilon_3 \quad (6c)$$

$$\gamma_4^2 = \beta^2 - k_4^2 = \beta^2 - \omega^2 \mu \epsilon_4 \quad (6d)$$

In Eq. (6),  $\varepsilon_1$ ,  $\varepsilon_2$ ,  $\varepsilon_3$  and  $\varepsilon_4$  are the dielectric constants, and  $\mu$  is the relative permeability of the medium. It should be remembered that  $n_i = \sqrt{\varepsilon_i}$ ,  $\varepsilon_i$  refers to the relative dielectric permittivity of medium  $i$ , and  $\beta$  is the longitudinal component of the propagation constant. Using the axial (or the longitudinal) components of the electric/magnetic fields, as described by Eqs. (2a)–(5b), the tangential field components in the different regions can be developed [27] as

$$E_{\rho 1} = \left\{ -C_1 \frac{j\beta}{q^2} \gamma_1 J'_\nu(\gamma_1 \rho) + C_2 \frac{\nu\omega\mu}{q^2 \rho} J_\nu(\gamma_1 \rho) \right\} e^{j\nu\phi} \quad (7a)$$

$$H_{\rho 1} = - \left\{ C_1 \frac{\nu\omega\varepsilon}{q^2 \rho} J_\nu(\gamma_1 \rho) + C_2 \frac{j\beta}{q^2} \gamma_1 J'_\nu(\gamma_1 \rho) \right\} e^{j\nu\phi} \quad (7b)$$

$$E_{\phi 1} = \left\{ C_1 \frac{\beta\nu}{q^2 \rho} J_\nu(\gamma_1 \rho) + C_2 \frac{j\omega\mu}{q^2} \gamma_1 J'_\nu(\gamma_1 \rho) \right\} e^{j\nu\phi} \quad (8a)$$

$$H_{\phi 1} = \left\{ -C_1 \frac{j\omega\varepsilon}{q^2} \gamma_1 J'_\nu(\gamma_1 \rho) + C_2 \frac{\beta\nu}{q^2 \rho} J_\nu(\gamma_1 \rho) \right\} e^{j\nu\phi} \quad (8b)$$

$$E_{\rho 2} = \left\{ -C_3 \frac{j\beta}{q^2} \gamma_2 J'_\nu(\gamma_2 \rho) - C_4 \frac{j\beta}{q^2} \gamma_2 Y'_\nu(\gamma_2 \rho) \right. \\ \left. + C_5 \frac{\nu\omega\mu}{q^2 \rho} J_\nu(\gamma_2 \rho) + C_6 \frac{\nu\omega\mu}{q^2 \rho} Y_\nu(\gamma_2 \rho) \right\} e^{j\nu\phi} \quad (9a)$$

$$H_{\rho 2} = - \left\{ C_3 \frac{\omega\varepsilon\nu}{q^2 \rho} J_\nu(\gamma_2 \rho) + C_4 \frac{\omega\varepsilon\nu}{q^2 \rho} Y_\nu(\gamma_2 \rho) \right. \\ \left. + C_5 \frac{j\beta}{q^2} \gamma_2 J'_\nu(\gamma_2 \rho) + C_6 \frac{j\beta}{q^2} \gamma_2 Y'_\nu(\gamma_2 \rho) \right\} e^{j\nu\phi} \quad (9b)$$

$$E_{\phi 2} = \left\{ C_3 \frac{\beta\nu}{q^2 \rho} J_\nu(\gamma_2 \rho) + C_4 \frac{\beta\nu}{q^2 \rho} Y_\nu(\gamma_2 \rho) \right. \\ \left. + C_5 \frac{j\omega\mu}{q^2} \gamma_2 J'_\nu(\gamma_2 \rho) + C_6 \frac{j\omega\mu}{q^2} \gamma_2 Y'_\nu(\gamma_2 \rho) \right\} e^{j\nu\phi} \quad (10a)$$

$$H_{\phi 2} = \left\{ -C_3 \frac{j\omega\varepsilon}{q^2} \gamma_2 J'_\nu(\gamma_2 \rho) - C_4 \frac{j\omega\varepsilon}{q^2} \gamma_2 Y'_\nu(\gamma_2 \rho) \right. \\ \left. + C_5 \frac{\beta\nu}{q^2 \rho} J_\nu(\gamma_2 \rho) + C_6 \frac{\beta\nu}{q^2 \rho} Y_\nu(\gamma_2 \rho) \right\} e^{j\nu\phi} \quad (10b)$$

$$E_{\rho 3} = \left\{ -C_7 \frac{j\beta}{q^2} \gamma_3 K'_\nu(\gamma_3 \rho) - C_8 \frac{j\beta}{q^2} \gamma_3 H_\nu^{(1)'}(\gamma_3 \rho) + C_9 \frac{\nu\omega\mu}{q^2 \rho} K_\nu(\gamma_3 \rho) + C_{10} \frac{\nu\omega\mu}{q^2 \rho} H_\nu^{(1)}(\gamma_3 \rho) \right\} e^{j\nu\phi} \quad (11a)$$

$$H_{\rho 3} = - \left\{ C_7 \frac{\nu\omega\varepsilon}{q^2 \rho} K_\nu(\gamma_3 \rho) + C_8 \frac{\nu\omega\varepsilon}{q^2 \rho} H_\nu^{(1)}(\gamma_3 \rho) + C_9 \frac{j\beta}{q^2} \gamma_3 K'_\nu(\gamma_3 \rho) + C_{10} \frac{j\beta}{q^2} \gamma_3 H_\nu^{(1)'}(\gamma_3 \rho) \right\} e^{j\nu\phi} \quad (11b)$$

$$E_{\phi 3} = \left\{ C_7 \frac{\beta\nu}{q^2 \rho} K_\nu(\gamma_3 \rho) + C_8 \frac{\beta\nu}{q^2 \rho} H_\nu^{(1)}(\gamma_3 \rho) + C_9 \frac{j\omega\mu}{q^2} \gamma_3 K'_\nu(\gamma_3 \rho) + C_{10} \frac{j\omega\mu}{q^2} \gamma_3 H_\nu^{(1)'}(\gamma_3 \rho) \right\} e^{j\nu\phi} \quad (12a)$$

$$H_{\phi 3} = \left\{ -C_7 \frac{j\omega\varepsilon}{q^2} \gamma_3 K'_\nu(\gamma_3 \rho) - C_8 \frac{j\omega\varepsilon}{q^2} \gamma_3 H_\nu^{(1)'}(\gamma_3 \rho) + C_9 \frac{\beta\nu}{q^2 \rho} K_\nu(\gamma_3 \rho) + C_{10} \frac{\beta\nu}{q^2 \rho} H_\nu^{(1)}(\gamma_3 \rho) \right\} e^{j\nu\phi} \quad (12b)$$

$$E_{\rho 4} = \left\{ -C_{11} \frac{j\beta}{q^2} \gamma_4 K'_\nu(\gamma_4 \rho) + C_{12} \frac{\nu\omega\mu}{q^2 \rho} K_\nu(\gamma_4 \rho) \right\} e^{j\nu\phi} \quad (13a)$$

$$H_{\rho 4} = - \left\{ C_{11} \frac{\nu\omega\varepsilon}{q^2 \rho} K_\nu(\gamma_4 \rho) + C_{12} \frac{j\beta}{q^2} \gamma_4 K'_\nu(\gamma_4 \rho) \right\} e^{j\nu\phi} \quad (13b)$$

$$E_{\phi 4} = \left\{ C_{11} \frac{\beta\nu}{q^2 \rho} K_\nu(\gamma_4 \rho) + C_{12} \frac{j\omega\mu}{q^2} \gamma_4 K'_\nu(\gamma_4 \rho) \right\} e^{j\nu\phi} \quad (14a)$$

$$H_{\phi 4} = \left\{ -C_{11} \frac{j\omega\varepsilon}{q^2} \gamma_4 K'_\nu(\gamma_4 \rho) + C_{12} \frac{\beta\nu}{q^2 \rho} K_\nu(\gamma_4 \rho) \right\} e^{j\nu\phi} \quad (14b)$$

In Eqs. (7a)–(14b), prime represents the differentiation with respect to the argument, and the parameter  $q$  is defined as

$$q^2 = k^2 - \beta^2 = \omega^2 \mu \varepsilon - \beta^2 \quad (15)$$

The continuity conditions require that the tangential components of the electric field  $E$  and the magnetic field  $H$  must be smooth at the different layer interfaces. As there are three interfaces in the fiber, there can be twelve equations altogether when the boundary conditions are matched at the layer interfaces with the parametric coordinates  $\rho = \rho_1$ ,  $\rho = \rho_2$  and  $\rho = \rho_3$ . Those equations are not presented in the

paper keeping in mind the length of the equations. In order to have the equations to be consistent, the determinant ( $\Delta_1$ ) formed by the coefficients of those equations must vanish, i.e.,

$$\Delta_1 = 0 \quad (16)$$

The explicit form of  $\Delta_1$ , which is a  $12 \times 12$  determinant, is also not incorporated into the paper. Eq. (16) illustrates the eigenvalue equation for the four-layer fiber with Au nano-coating. The solutions to Eq. (16) will provide the allowed values of the propagation constants of modes sustained in the fiber. The left hand side of Eq. (16) is complex in nature, and therefore, this equation may be rewritten as

$$\Delta_{11} + j\Delta_{12} = 0 \quad (17)$$

where  $\Delta_{11}$  and  $\Delta_{12}$ , respectively, represent the real and the imaginary parts of  $\Delta_1$ . In order to get the solutions of Eq. (17), both the real and the imaginary parts must be zero at the same time, and the corresponding values of  $\beta$  will represent the propagation constants of the sustained modes.

## 2.2. Case II: Fiber without Au-coating (Three-layer Fiber)

For three-layer dielectric fibers, the electric/magnetic fields in the central core section can be taken in the form of Bessel function  $J_\nu(\cdot)$  of the first kind, whereas those in the inner clad can be represented by the linear combination of Bessel functions of the first and the second kinds, i.e.,  $J_\nu(\cdot)$  and  $Y_\nu(\cdot)$ . In the outer clad section, field essentially has decaying character with increasing radial parameter, and therefore, the most suitable solution in this region can be represented by the modified Bessel function  $K_\nu(\cdot)$  of the second kind. The axial components of the electric/magnetic fields (i.e.,  $E_z$  and  $H_z$ ) for the different regions of the fiber can be written on the basis of these considerations. Those axial components can be used to determine the transverse field components (i.e.,  $E_\rho$ ,  $H_\rho$  and  $E_\phi$ ,  $H_\phi$ ) corresponding to the different regions of the fiber. These field components are not explicitly stated in the text, but used to develop the equations that can be obtained after implementing the continuity conditions at the layer interfaces. As there are two interfaces in the fiber, there can be eight equations generated altogether after implementing the boundary conditions at the layer interfaces with the parametric coordinates  $\rho = a$  and  $\rho = b$  (with  $a < b$ ). In order to simplify the situation, the outermost region is considered to be infinitely extended. The form of this set of eight equations is as

follows:

$$A_1 J_\nu(\gamma_1 a) - A_3 J_\nu(\gamma_2 a) - A_4 Y_\nu(\gamma_2 a) = 0 \quad (18)$$

$$A_2 J_\nu(\gamma_1 a) - A_5 J_\nu(\gamma_2 a) - A_6 Y_\nu(\gamma_2 a) = 0 \quad (19)$$

$$A_1 \frac{\beta\nu}{q_1^2 a} J_\nu(\gamma_1 a) + A_2 \frac{j\omega\mu}{q_1^2} \gamma_1 J'_\nu(\gamma_1 a) - A_3 \frac{\beta\nu}{q_2^2 a} J_\nu(\gamma_2 a) - A_4 \frac{\beta\nu}{q_2^2 a} Y_\nu(\gamma_2 a) - A_5 \frac{j\omega\mu}{q_2^2} \gamma_2 J'_\nu(\gamma_2 a) - A_6 \frac{j\omega\mu}{q_2^2} \gamma_2 Y'_\nu(\gamma_2 a) = 0 \quad (20)$$

$$- A_1 \frac{j\omega\varepsilon}{q_1^2} \gamma_1 J'_\nu(\gamma_1 a) + A_2 \frac{\beta\nu}{q_1^2 a} J_\nu(\gamma_1 a) + A_3 \frac{j\omega\varepsilon}{q_2^2} \gamma_2 J'_\nu(\gamma_2 a) + A_4 \frac{j\omega\varepsilon}{q_2^2} \gamma_2 Y'_\nu(\gamma_2 a) - A_5 \frac{\beta\nu}{q_2^2 a} J_\nu(\gamma_2 a) - A_6 \frac{\beta\nu}{q_2^2 a} Y_\nu(\gamma_2 a) = 0 \quad (21)$$

$$A_3 J_\nu(\gamma_2 b) + A_4 Y_\nu(\gamma_2 b) - A_7 K_\nu(\gamma_3 b) = 0 \quad (22)$$

$$A_5 J_\nu(\gamma_2 b) + A_6 Y_\nu(\gamma_2 b) - A_8 K_\nu(\gamma_3 b) = 0 \quad (23)$$

$$A_3 \frac{\beta\nu}{q_2^2 b} J_\nu(\gamma_2 b) + A_4 \frac{\beta\nu}{q_2^2 b} Y_\nu(\gamma_2 b) + A_5 \frac{j\omega\mu}{q_2^2} \gamma_2 J'_\nu(\gamma_2 b) + A_6 \frac{j\omega\mu}{q_2^2} \gamma_2 Y'_\nu(\gamma_2 b) - A_7 \frac{\beta\nu}{q_3^2 b} K_\nu(\gamma_3 b) - A_8 \frac{j\omega\mu}{q_3^2} \gamma_3 K'_\nu(\gamma_3 b) = 0 \quad (24)$$

$$- A_3 \frac{j\omega\varepsilon}{q_2^2} \gamma_2 J'_\nu(\gamma_2 b) - A_4 \frac{j\omega\varepsilon}{q_2^2} \gamma_2 Y'_\nu(\gamma_2 b) + A_5 \frac{\beta\nu}{q_2^2 b} J_\nu(\gamma_2 b) + A_6 \frac{\beta\nu}{q_2^2 b} Y_\nu(\gamma_2 b) + A_7 \frac{j\omega\varepsilon}{q_3^2} \gamma_3 K'_\nu(\gamma_3 b) - A_8 \frac{\beta\nu}{q_3^2 b} K_\nu(\gamma_3 b) = 0 \quad (25)$$

In Eqs. (18)–(25),  $A_1 - A_8$  are unknown constants to be determined by the boundary conditions. Also,  $\gamma_1$ ,  $\gamma_2$  and  $\gamma_3$  are the quantities as defined in Eq. (6). For Eqs. (18)–(25) to be consistent, the determinant ( $\Delta_2$ ) formed by the coefficients  $A_1 - A_8$  must vanish, i.e.,

$$\Delta_2 = 0 \quad (26)$$

$\Delta_2$  is essentially a  $8 \times 8$  determinant, the explicit form of which is not incorporated into the text. Eq. (26) determines the dispersion relation for the three-layer dielectric fiber without Au-coating, the solutions of which will provide the actual values of modal propagation constants satisfied by the fiber. Once again the form of  $\Delta_2$  is complex, and therefore, one may rewrite Eq. (26) as

$$\Delta_{21} + j\Delta_{22} = 0 \quad (27)$$

where  $\Delta_{21}$  and  $\Delta_{22}$  are, respectively, the real and the imaginary parts of  $\Delta_2$ . Obviously, the valid propagation constants of the sustained

modes in the fiber will be only those for which both  $\Delta_{21}$  and  $\Delta_{22}$  simultaneously vanish.

### 3. RESULTS AND DISCUSSION

On the basis of the eigenvalue Eq. (17), it will be rather interesting to analytically study the modal properties which would give an insight into the propagation characteristics of fibers having Au nano-layer coating. For the sake of comparison, the eigenvalue Eq. (27) is also considered, which corresponds to the case of three-layer dielectric fibers. As we used Maxwell's equations for the development of dispersion relations, the analysis becomes much rigorous, and we identify the obtained modes as transverse electric (TE) and hybrid EH modes.

In our numerical computation, the operating wavelength  $\lambda$  is taken to be 850 nm, which falls in the visible region of the EM spectrum. We consider the RI values  $n_1$  and  $n_2$  as 1.4488 and 1.444, respectively. Also, the Au-coated layer has the RI as  $n_3 = 1.42$ . Further, the parametric boundaries  $\rho_1$  and  $\rho_2$  are taken to be 4.1  $\mu\text{m}$  and 62.5  $\mu\text{m}$ , respectively, and the outermost layer is assumed to be infinitely extended. With these parameters, the results are obtained for varying Au-layer thickness  $\rho_3$  under the consideration that all the regions are non-magnetic in nature ( $\mu_1 = \mu_2 = \mu_3 = \mu_4 \approx \mu_0$ , i.e., the relative permeability of the free-space).

Figure 1 shows the logarithmic plots of the real ( $\Delta_{11}$ ) and the imaginary ( $\Delta_{12}$ ) parts of the eigenvalue Eq. (17) against the propagation constant  $\beta$ , the values of which are limited by the condition of sustained guidance, i.e.,  $n_1k \geq \beta \geq n_2k$ ;  $k$  being the free-space propagation constant. These plots are obtained corresponding to the azimuthal mode index  $\nu = 0$ , and the Au nano-layer thickness  $\delta (= \rho_3 - \rho_2)$  as 20 nm. We observe that the curves are oscillatory in nature, and simultaneous intersection of the two curves (corresponding to  $\Delta_{11}$  and  $\Delta_{12}$ , as shown by solid and dashed lines, respectively, in Fig. 1) with the horizontal axis will provide the solutions to the Eq. (17), or in other words, the modes supported by the fiber. In this way, approximate values of the propagation constants of the sustained modes may also be estimated. We observe from Fig. 1 that there are some thirteen TE modes sustained in the fiber structure with different values of propagation constants.

In order to observe the effect of the Au-layer thickness on the number of sustained modes, we repeated the computation for different values of  $\delta$ , namely 20 nm, 50 nm, 100 nm, 150 nm, and 200 nm. However, in the paper, we incorporated the illustrative logarithmic

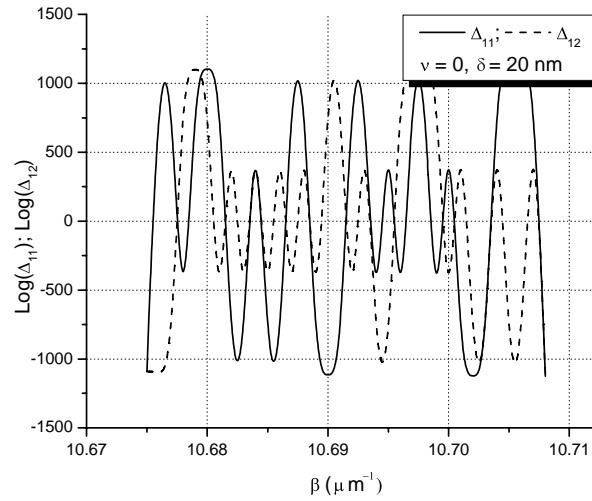


**Figure 1.** Logarithmic plots of  $\Delta_{11}$  and  $\Delta_{12}$  against  $\beta$  for TE modes with 20 nm Au coating thickness.

plots of the real and the imaginary parts corresponding to  $\delta = 20$  nm and 150 nm only. In the case of  $\delta = 150$  nm, we observe from Fig. 2 that the number of sustained TE modes is much reduced; approximately seven modes are supported by the fiber. This is essentially attributed to the increased Au-layer thickness in this case, when the fiber attains the mode-suppression property owing to having loaded with a metallic layer. With further increased value of the Au-layer thickness, viz.  $\delta = 200$  nm, the number of supported modes can be seen as further reduced, and in this case, it can be observed that approximately five modes are sustained within the fiber (the relevant plot is not incorporated into the text). As stated before, the phenomenon of reduction of the number of sustained modes is due to the enhanced thickness of the Au nano-layer.

From the inspection of the joint intersection of the real and the imaginary parts (of Eq. (17)) with the  $\beta$ -axis in Figs. 1 and 2, one may estimate the propagation constants of the different TE modes supported in the fiber. The Au coating layer essentially has its profound effect on the number of propagation modes. In order to have a look at the trend of the variation in the propagation constants of the modes with the Au-layer thickness, a plot of Fig. 3 is performed illustrating the cases of the first three TE modes, viz.  $TE_{01}$ ,  $TE_{02}$  and  $TE_{03}$ . We observe that, for all the three types of modes, the  $\beta$ -values are relatively small corresponding to the situation when the Au-layer

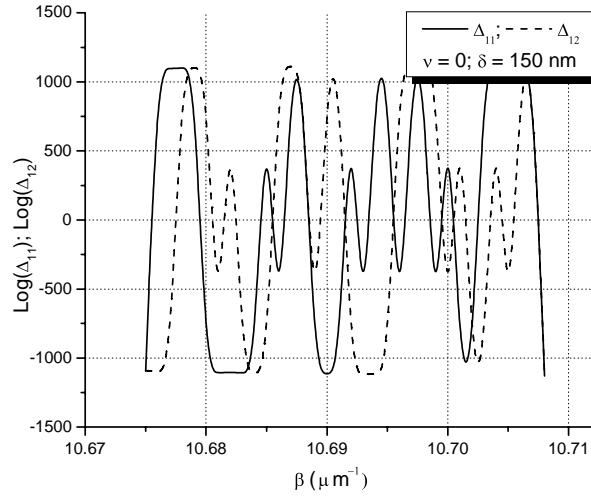


**Figure 2.** Logarithmic plots of  $\Delta_{11}$  and  $\Delta_{12}$  against  $\beta$  for TE modes with 150 nm Au coating thickness.

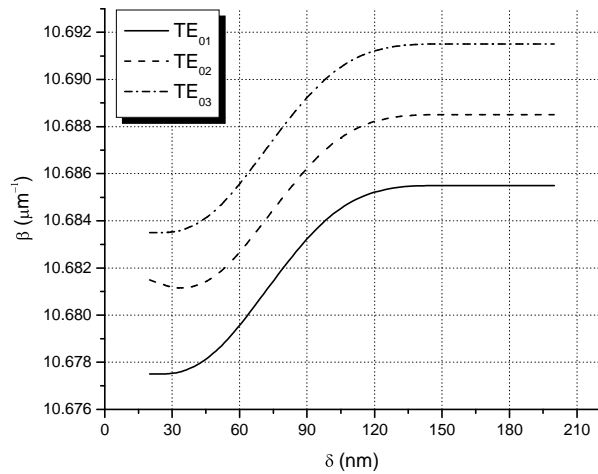


**Figure 3.** Variation of the propagation constants of TE modes with the nano-coating thickness.

thickness is small. These ( $\beta$ -values) show an initial rise in their values with increasing layer thickness, and then become almost constant with further increase in the thickness values. We also observe that the lowest mode ( $TE_{01}$ ) has the least value of propagation constant, which is very much obvious so far as the phenomenon of wave propagation

in bounded medium is concerned. The trend of the variation of the propagation constant with the nano-coating thickness may be attributed to the size of Au nano-particles. It may be considered that, with the increase in the nano-coating thickness, the Au nano-particles would acquire larger size owing to their greater accumulation. This, in turn, affects the modal confinement in the nano-layer, and with the increase in the nano-layer thickness, their propagation gets almost saturated. A thorough investigation in this regard is currently underway, and is expected to be taken up in a future communication after the Au nano-particle deposition chemistry is well-understood.

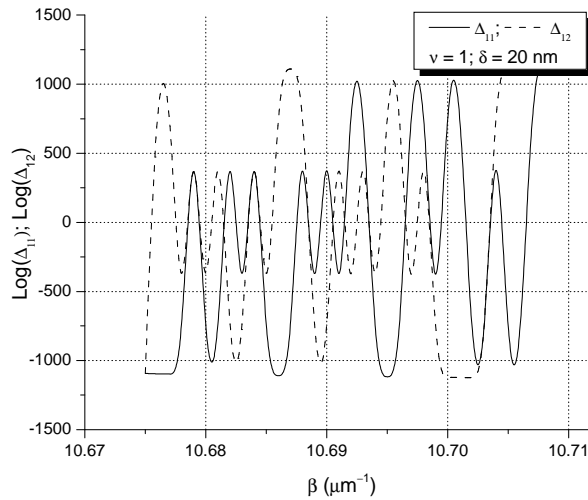


**Figure 4.** Logarithmic plots of  $\Delta_{11}$  and  $\Delta_{12}$  against  $\beta$  for EH modes with 20 nm Au coating thickness.

We performed the computation for hybrid modes too for which the azimuthal mode index  $\nu = 1$ . In this case also we considered the situations with different values of  $\delta$ , namely 20 nm, 50 nm, 100 nm, 150 nm, and 200 nm. Figs. 4 and 5, respectively, show the plots of  $\Delta_{11}$  and  $\Delta_{12}$  against the propagation constant  $\beta$  for the values of  $\delta$  as 20 nm and 200 nm. The other parameters related to fiber are left unchanged. We observe that the number of sustained modes in the fiber is relatively higher corresponding to the situation when the Au-layer thickness  $\delta$  is small. With the increase in  $\delta$ , the number of modes supported by the fiber is much reduced, e.g., when  $\delta = 200$  nm, approximately six modes are found to be sustained within the structure. As such, the effect of metallic loading once again becomes prominent because of which the fiber attains a mode-suppression property. However, in general, the

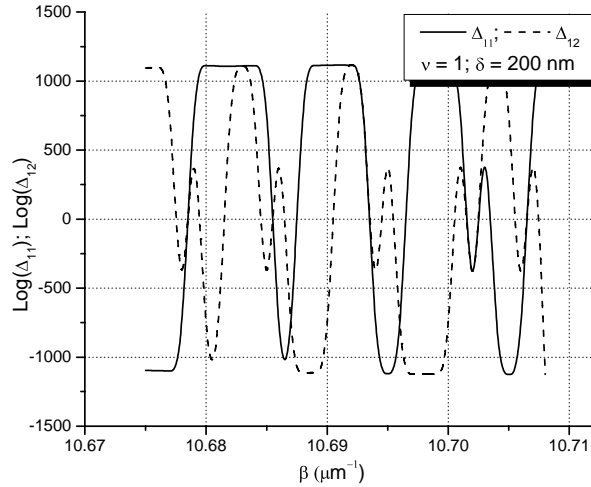


**Figure 5.** Logarithmic plots of  $\Delta_{11}$  and  $\Delta_{12}$  against  $\beta$  for EH modes with 200 nm Au coating thickness.

analyses indicate that the number of skew modes in the fiber is a little more than the number of sustained meridional modes.

In order to visualize the effect of Au-layer thickness  $\delta$  upon the values of the modal propagation constants  $\beta$ , a  $\delta$ - $\beta$  plot corresponding to hybrid EH modes is presented in Fig. 6. We observe that there is hardly any effect of the Au-layer thickness on the propagation constant for the  $\text{EH}_{11}$  mode. However, for the higher order  $\text{EH}_{12}$  and  $\text{EH}_{13}$  modes, the propagation constants increase with increasing  $\delta$  although the variation in their values is only marginal. Another aspect to be observed is that the attainment of saturation in  $\beta$ -values with increasing  $\delta$  is not prominently noticed in this case, which is in contrast to the case of meridional modes (Fig. 3) where the modal propagation constants corresponding to  $\text{TE}_{01}$ ,  $\text{TE}_{02}$  and  $\text{TE}_{03}$  modes are found to be getting saturated with the increase in Au-layer thickness.

At this stage of analysis, it would be of curiosity to observe the overall effect of loading an Au nano-layer over the dielectric fiber. In such attempt, a short discussion on the propagation behavior of three-layer fiber would be vital. To touch upon this aspect, logarithmic plots of the real ( $\Delta_{21}$ ) and the imaginary ( $\Delta_{22}$ ) parts of the eigenvalue Eq. (27) may be considered. The explicit forms of  $\Delta_{21}$  and  $\Delta_{22}$  are not incorporated into the text owing to their widely extended forms. In our computation, the parametric values related to the fiber are taken as  $n_1 = 1.4488$ ,  $n_2 = 1.444$ ,  $n_3 = 1$  (i.e., free-space),  $a = 4.1 \mu\text{m}$  and  $b = 62.5 \mu\text{m}$ . The operating wavelength  $\lambda$  is considered to be the

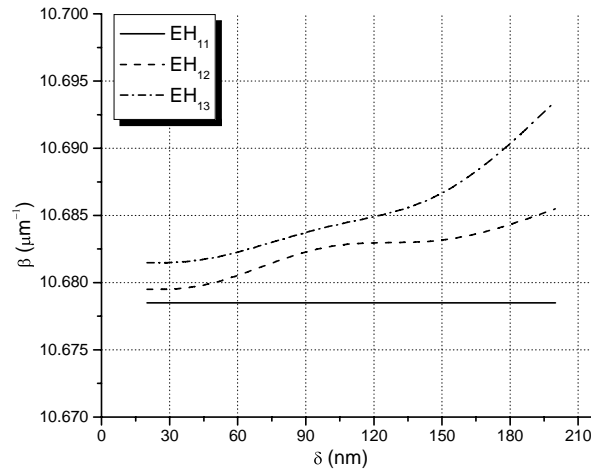


**Figure 6.** Variation of the propagation constants of EH modes with the nano-coating thickness.

same, i.e., 850 nm. Assuming non-magnetic behavior of the different fiber regions, such logarithmic plots of  $\Delta_{21}$  and  $\Delta_{22}$  are shown in Figs. 7 and 8 corresponding to TE and EH modes, respectively. These curves are also found to be oscillatory, and we observe from the crossings of  $\Delta_{21}$  and  $\Delta_{22}$  in Fig. 7 that the fiber roughly supports only four TE modes, which is less than those noticed in the case of Au-coated fiber. Fig. 8 indicates that the fiber sustains only about five EH modes. As such, the loading of an Au nano-layer over a dielectric fiber has generally the tendency of increasing the number of propagation modes in the fiber.

We now look at the values of propagation constants of TE and EH modes corresponding to the three-layer dielectric fiber, and compare those obtained with the Au-coated fiber. Comparing Figs. 3 and 8 we observe that, corresponding to the  $TE_{01}$  mode (for three-layer fiber; Fig. 7), it has the  $\beta$ -value vary close to that with the Au-coated fiber having the nano-layer thickness around 100 nm. Further, the hybrid  $EH_{11}$  mode travels in the three-layer fiber with the propagation constant which is almost equal to that corresponding to the Au-coated fiber with 50 nm thick coating (Fig. 6). Thus, the general observation would be that the loading of an additional Au nano-layer (on a three-layer dielectric fiber) has its effect to reduce the propagation constants of the sustained modes. However, this effect generally disappears with the increase in coating thickness.

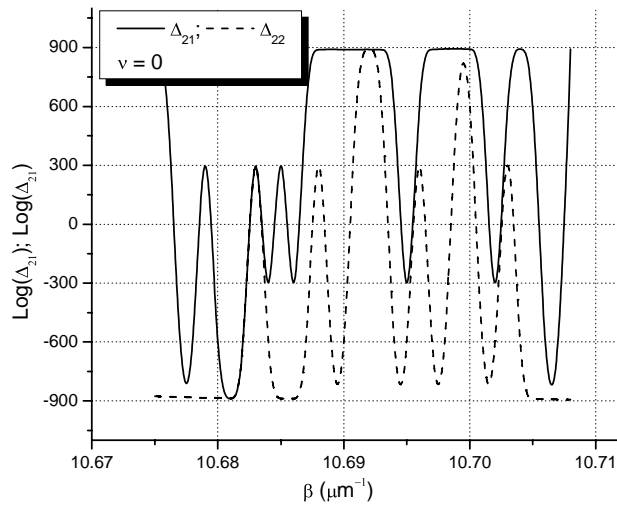


**Figure 7.** Logarithmic plots of  $\Delta_{21}$  and  $\Delta_{22}$  against  $\beta$  corresponding to TE modes.

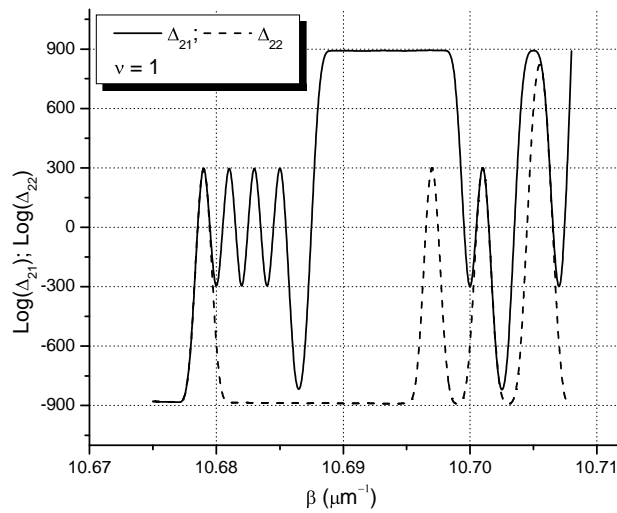


**Figure 8.** Logarithmic plots of  $\Delta_{21}$  and  $\Delta_{22}$  against  $\beta$  corresponding to EH modes.

#### 4. CONCLUSION

On the basis of forgoing analysis, the general inference may be drawn that the Au-coated fiber attains a mode suppression property with the increase in Au-layer thickness. Also, the propagation constants of the sustained modes greatly depend on the thickness of the Au-layer; the dependence is more profound corresponding to larger Au-layer thickness. We observed the cases of TE and EH modes, and it is noticed that the propagation constants of TE modes vary more (with the Au-layer thickness) as compared to those of the EH modes, although the higher order EH modes present a marginal increase in their propagation constant values (with increasing Au-layer thickness). Upon comparing the modal properties with that of the three-layer dielectric fiber, it is observed that the additional loading of the Au nano-layer enhances the number of propagation modes, though the sustained modes become lesser with increasing thickness of the Au coating. Further, the Au-layer has the effect to reduce the propagation constants of the sustained modes, which is more pronounced when the Au-layer thickness is relatively small; corresponding to intermediate (15  $\mu\text{m}$ –135  $\mu\text{m}$ ) Au-layer thickness, this effect is generally not that remarkable. As is well-known, the mode-suppression property of singly clad fibers generally deteriorates with the addition of more cladding, the similar feature is observed in the type of fibers considered in this communication.

#### ACKNOWLEDGMENT

This work was supported in part by the Ministry of Science, Technology and Innovation (Malaysia) under the eScience Fund Grant 03-02-01-SF0083, and the authors gratefully acknowledge the financial support received from the Govt. of Malaysia. The authors are greatly indebted to three anonymous reviewers for making constructive criticisms to enrich the work.

#### REFERENCES

1. Bhattacharjee, S., V. J. Menon, and K. K. Dey, "On the cutoff conditions and power distribution in fibers of arbitrary cross-section," *Can. J. Phys.*, Vol. 69, 612–615, 1990.
2. Ono, K. and H. Osawa, "Excitation characteristics of fundamental mode in tapered slab waveguides with nonlinear cladding," *Electron. Lett.*, Vol. 27, 664–666, 1991.

3. Choudhury, P. K. and O. N. Singh, "Some multilayered and other unconventional lightguides," *Electromagnetic Fields in Unconventional Materials and Structures*, Chapt. 8, John Wiley and Sons, New York, 2000.
4. Choudhury, P. K. and T. Yoshino, "TE and TM modes power transmission through liquid crystal optical fibers," *Optik*, Vol. 115, 49–56, 2004.
5. Nair, A. and P.K. Choudhury, "On the analysis of field patterns in chirofibers," *J. Electromag. Waves and Appl.*, Vol. 21, 2277–2286, 2007.
6. Ibrahim, A.B. M. A. and P. K. Choudhury, "Relative power distributions in omniguiding photonic band-gap fibers," *Progress In Electromagnetics Research*, PIER 72, 269–278, 2007.
7. Cheng, Q. and T.-J. Cui, "Guided modes and continuous modes in parallel-plate waveguides excited by a line source," *J. Electromag. Waves and Appl.*, Vol. 21, 1577–1587, 2007.
8. Mei, Z.-L. and F.-Y. Xu, "A simple, fast and accurate method for calculating cutoff wavelengths for the dominant mode in elliptical waveguide," *J. Electromag. Waves and Appl.*, Vol. 21, 367–374, 2007.
9. Kumar, D., P. K. Choudhury, and F. A. Rahman, "Towards the characteristic dispersion relation for step-index hyperbolic waveguide with conducting helical winding," *Progress In Electromagnetics Research*, PIER 71, 251–275, 2007.
10. Kumar, D., P. K. Choudhury, and O. N. Singh II, "Towards the dispersion relations for dielectric optical fibers with helical windings under slow- and fast-wave considerations — A comparative analysis," *Progress In Electromagnetics Research*, PIER 80, 409–420, 2008.
11. Kawakami, S. and S. Nishida, "Characteristics of a doubly clad optical fiber with a low index inner cladding," *IEEE J. Quantum Electron.*, Vol. 10, 879–887, 1974.
12. Borland, W. C., D. E. Zelmon, C. J. Radens, J. T. Boyd, and H. E. Jackson, "Properties of four-layer planar optical waveguides near cutoff," *IEEE J. Quantum Electron.*, Vol. 23, 1172–1179, 1978.
13. Chaubey, V. K., K. K. Dey, S. P. Ojha, and P. Khastgir, "Modal characteristics of a doubly clad step-index fiber: A general analytical study," *Can. J. Phys.*, Vol. 66, 796–802, 1988.
14. Choudhury, P. K. and R. A. Lessard, "An estimation of power transmission through a doubly clad optical fiber with annular

- core,” *Microw. and Opt. Tech. Lett.*, Vol. 29, 402–405, 2001.
15. Takeo, T. and H. Hattori, “Optical fiber sensor for measuring refractive index,” *Jpn. J. Appl. Phys.*, Vol. 21, 1509–1512, 1982.
  16. Paul, P. H. and G. Kychakoff, “Fiber-optic evanescent field absorption sensor,” *Appl. Phys. Lett.*, Vol. 51, 12–14, 1987.
  17. Messica, A., A. Greenstein, and A. Katzir, “Theory of fiber-optic evanescent-wave spectroscopy and sensors,” *Appl. Opt.*, Vol. 35, 2274–2284, 1996.
  18. Choudhury, P. K. and O. N. Singh, “An overview of optical sensors and their applications,” *Frontiers in Optical Technology: Materials and Devices*, Chapt. 9, Nova Science Publisher, New York, 2007.
  19. Suyama, T., Y. Okuno, A. Matsushima, and M. Ohtsu, “A numerical analysis of stop band characteristics by multilayered dielectric gratings with sinusoidal profile,” *Progress In Electromagnetics Research B*, Vol. 2, 83–102, 2008.
  20. Cheng, S. F. and L. K. Chau, “Colloidal gold-modified optical fiber for chemical and biochemical sensing,” *Anal. Chem.*, Vol. 75, 16–21, 2003.
  21. Sharma, A. K., R. Jha, and B. D. Gupta, “Fiber-optic sensors based on surface plasmon resonance: A comprehensive review,” *IEEE Sensors J.*, Vol. 7, 1118–1129, 2007.
  22. Lee, C.C. and S. Chi, “Measurement of stimulated-Brillouin-scattering threshold for various types of fibers using Brillouin optical-time-domain reflectometer,” *IEEE Phot. Technol. Lett.*, Vol. 12, 672–674, 2000.
  23. Lee, C.C., P.W. Chiang, and S. Chi, “Utilization of a dispersion-shifted fiber for simultaneous measurement of distributed strain and temperature through Brillouin frequency shift,” *IEEE Phot. Technol. Lett.*, Vol. 13, 1094–1096, 2001.
  24. Zou, W., Z. He, M. Kishi, and K. Hotate, “Stimulated Brillouin scattering and its dependences on temperature and strain in a high-delta optical fiber with F-doped depressed inner cladding,” *Opt. Lett.*, Vol. 32, 600–602, 2007.
  25. Sjöberg, D., “Determination of propagation constants and material data from waveguide measurements,” *Progress In Electromagnetics Research B*, Vol. 12, 163–182, 2009.
  26. Abramowitz, M. and I. A. Stegun, *Handbook of Mathematical Functions*, Chap. 9, Dover Publications, Inc., New York, 1965.
  27. Keiser, G., *Optical Fiber Communications*, Chap. 2, McGraw-Hill, Singapore, 1986.